ORIGINAL PAPER

**V. D. Jović · B. M. Jović · M. G. Pavlović ·
V. Maksimović**

Morphology and composition of Ni–Co alloy powders electrodeposited from ammoniacal electrolyte

Abstract In this paper, the morphology and phase structure of Ni–Co powders electrodeposited from ammoniacal electrolyte are investigated as a function of alloy powder composition. Composition of the electrolyte, i.e. the ratio of Ni^{2+}/Co^{2+} concentration is found to influence both, the phase structure and the morphology of Ni–Co alloy powders. It is shown that the current density practically does not influence the morphology of Ni–Co alloy powders as well as alloy powder composition. At the highest ratio of the Ni^{2+}/Co^{2+} ions typical spongy particles were obtained. With the decrease of the Ni^{2+}/Co^{2+} ions ratio agglomerates of the size of about 100 μm, composed of a large number of fern-like dendrites on their surface were obtained. At the lowest Ni^{2+}/Co^{2+} concentration ratio, among more dendritic particles, agglomerates typical for pure Co powder deposition were detected. It is also shown that depending on the Ni^{2+}/Co^{2+} ratio different types of Ni and Co codeposition could be detected: anomalous and irregular. At the Ni^{2+}/Co^{2+} ions ratio higher than 1 only β-Ni phase was detected, while at concentration ratios $Ni^{2+}/Co^{2+} < 1$ h.c.p. α-Co phase together with β-Ni phase was detected in the alloy powder deposit.

Keywords Ni-Co powders · Fern-like dendrites · Different agglomerates · f.c.c. β-Ni phase · h.c.p. α-Co phase

V. D. Jović · B. M. Jović
Center for Multidisciplinary Studies, University of Belgrade,
P. O. Box 33, 11030 Belgrade, Serbia and Montenegro

M. G. Pavlović (✉)
ICTM, Institute of Electrochemistry, Njegoševa 12,
11000 Belgrade, Serbia and Montenegro
E-mail: duki@elab.tmf.bg.ac.yu
Tel.: +381-11-3370430
Fax: +381-11-3370389

V. Maksimović
Institute of Nuclear Science, , "Vinča",
P. O. Box 522, Belgrade, Serbia and Montenegro

Introduction

Almost all materials can be made into powder, but the method selected for producing a powder depends on the specific material properties. Depending on the shape of the product, initial powders have to satisfy different requirements. These include physical, chemical and technological properties. The four main categories of fabrication techniques are based on mechanical comminuting, chemical reactions, electrolytic deposition and liquid metal atomization [1].

The electrolytic powder production method usually yields products of high purity, which can be well pressed and sintered. Besides, in recent years, it has been shown that by different electrolysis regimes it is possible, not only to obtain powders with a wide range of properties, but also to predict the decisive characteristics of powders, which are of vital importance for powder quality and for appropriate application [2].

Alloys of iron group metals, Fe, Ni and Co, are known as very good magnetic materials since 1921 [3–5]. It has long be known that $NiCo_2O_4$ is an active bifunctional catalysts for oxygen evolution [6, 7] and reduction [8, 9] in alkaline media. The powders of such oxide have been prepared by thermal decomposition of mixed nitrates, carbonates or hydroxides [10–12], sol-gel [13–15], freeze drying [16] or vacuum deposition method with subsequent thermal treatment [17]. Electrodeposited Ni–Co alloys were also used as catalysts for H_2O_2 decomposition [18].

Only a few papers concerning Ni–Co powder electrodeposition exist in the literature. Yur'ev et al. [19] proposed a new method for the electrodeposition of multicomponent powders using Ni–Co alloy as an example. The principal improvement represents the use of two independent anodes (Ni and Co) with separately controlled current densities. To achieve this they had to use chloride-containing electrolyte (NH_4Cl and NaCl) to provide dissolution of Ni and Co anodes in order to keep constant concentration of Ni and Co ions in the

Table 1 Parameters of different phases shown in Fig. 1

Sample	Observed d (Å)	Standard d (Å)	Phases		hkl	2θ	Crystallite size[a] (nm)	Lattice distortion[a] (%)
			fcc	Hcp				
Fig. 3a	2,038	2,034	β-Ni		111	44,415	23.7	0.092
	1,7634	1,762	β-Ni		200	51,803		
	1,2460	1,246	β-Ni		220	76,373		
	1,0631	1,0624	β-Ni		311	92,867		
Fig. 3b	2,0320	2,034	β-Ni		111	44,533	27.7	0.079
	1,17619	1,762	β-Ni		200	51,850		
	1,246	1,246	β-Ni		220	76,373		
	1,0631	1,0624	β-Ni		311	92,867		
Fig. 3c	2,1585	2,165		α-Co	100	41,815	β-Ni	
	2,0329	2,034	β-Ni		111	44,534	30.9	0.071
	1,9093	1,91		α-Co	101	47,587	+	
	1,7618	1,762	β-Ni		200	51,853	α-Co	
	1,2467	1,246	β-Ni		220	76,322	16.5	0.12

[a]The crystallite size and lattice distortion are determined from FWHM

electrolyte. It was shown that powders could be obtained only at current densities higher than 3,000 A m^{-2}, with the optimal conditions of electrolysis being: Co^{2+} + Ni^{2+} = 16 g dm^{-3}, NH$_4$Cl 25 g dm^{-3}, NaCl 40 g dm^{-3}, pH = 3.5–5.0, cathode current density 5,000–20,000 A m^{-2}, anode current density for Co and Ni 100–200 A m^{-2}, temperature of the electrolyte 25°C. Ni–Co powders produced under such conditions were found to be solid solutions of Co and Ni. El-Halim et al. [18] investigated Ni–Co powder electrodeposition from the electrolyte containing sulfate and boric acid. It was found that with increasing concentration ratio of Ni^{2+}/Co^{2+} ions in the electrolyte (minimal concentration of Ni^{2+} ions was 0.0125 M) from 1/1 to 6/1 the content of Ni in the powder increases non-linearly from about 50% to about 85%. The increase of the ammonium sulfate concentration was found to change the morphology of the powder (at constant Ni^{2+}/Co^{2+} ratio 1/1) from clusters of nodular dendrites covering the whole surface of the cathode towards the formation of leaf-like outgrowths leaving holes between them. At relatively low current density of 3.3 A dm^{-2} individual coarse-grained particles were formed, while at higher current density of 10.0 A dm^{-2} gradual coalescence and refinement of the particles to form nodular clusters was achieved. X-ray investigation revealed that the as-deposited Ni-rich alloy, containing more than 51% of Ni, consist solely of the β-Ni phase with the f.c.c. structure of the orientations (111), (200) and (220), while Co-rich alloys consist of a mixture of the f.c.c. β-Ni phase and the h.c.p. α-Co phase.

In this paper, results on the investigation of the morphology and phase structure of Ni–Co alloy powders electrodeposited from ammoniacal electrolyte are presented and discussed.

Experimental

All powder samples were electrodeposited at the temperature of 50°C in the cylindrical glass cell of the total volume of 1 dm^3 with cone shaped bottom of the cell in order to collect powder particles in it. Working electrode was a glassy carbon rod of the diameter of 5 mm, with the total surface area of 7.5 cm^2 immersed in the solution and placed in the middle of the cell. Cylindrical Ni foil placed close to the cell walls was used as a counter electrode providing excellent current distribution in the cell. Electrodeposition of powders was performed with a constant current regime using appropriate power supply. The deposition time was usually 2 h providing that the total concentration of the metal ions in the solution did not change more than 10% and that the amount of electrodeposited powder was enough for SEM, X-ray and composition analysis. During the deposition process powder was removed from the electrode surface using gentle brush every 15–20 min. All solutions were made from distilled water and analytical grade chemicals. After deposition, powders were washed with distilled water and alcohol and left to dry in the air at room temperature.

X-ray powder diffraction (XRD) analysis of Ni–Co alloy powders was carried out by a Siemens D500 diffractometer with a Ni filter and CuK$_\alpha$ radiation operated at a tube voltage of 35 kV and a tube current of 20 mA. A step scan mode was utilized with 0.02° 2θ per step. The time step was 2 s. The angular 2θ range investigated was 5–100° (0.6° 2θ min^{-1}).

The morphology of the electrodeposited powders was examined using scanning electron microscope, SEM (Philips, model XL30).

EDS analysis was performed on SEM (JEOL JSM 6460LV)

Chemical analysis of the powder composition was performed by AAS using SPECTRO ICP-OES 17.5 MHz spectrometer. Samples for the analysis of about 30 µg were dissolved in 5 cm^3 HCl (1:1) at slightly elevated temperature. This procedure was repeated three times and the average value is given in the paper.

Four different Ni^{2+}/Co^{2+} concentration ratios were used for Ni–Co powders electrodeposition from the electrolyte containing Ni and Co sulfate salts and 1 M (NH$_4$)$_2$SO$_4$ + 0.7 NH$_4$OH: (1) Ni^{2+}/Co^{2+} = 4.00 (0.1 M NiSO$_4$/0.025 M CoSO$_4$); (2) Ni^{2+}/Co^{2+} = 1.50

(0.06 M NiSO$_4$/0.04 M CoSO$_4$); (3) Ni^{2+}/Co^{2+} = 0.67 (0.04 M NiSO$_4$/0.06 M CoSO$_4$) and (4) Ni^{2+}/Co^{2+} = 0.25 (0.025 M NiSO$_4$/0.1 M CoSO$_4$). pH of the investigated solutions varied between 9.2 and 9.5. Ni–Co alloys were deposited at three different current densities for each electrolyte composition: I 0.1 A cm^{-2}, III 0.3 A cm^{-2} and V 0.5 A cm^{-2}.

Results and discussion

It should be mentioned here that for all solutions (alloy compositions) the highest amount of the compact deposit, of about 85% was obtained at the lowest current density of 0.1 A cm^{-2}. At $j = 0.3$ A cm^{-2} more than 85% of the deposit was powder, while at $j = 0.5$ A cm^{-2} almost 100% of the deposit was obtained as a powder, while small amount of the deposit was always present on the electrode surface after the deposition. It is shown that the composition of the deposit is independent of the current density.

Polarization diagrams for Ni–Co alloy powder electrodeposition

In order to obtain polarization diagrams corresponding only to the process of Ni–Co alloy powder electrodeposition, it was necessary to correct measured polarization curves for IR drop and for hydrogen evolution current, since massive hydrogen evolution occurs during the process of alloy powder electrodeposition. The procedure that was used to obtain such polarization diagrams is explained in details in our next paper (V.D. Jović, B.M. Jović, M.G. Pavlović, in preparation). In Fig. 1a shows the polarization curves corresponding to

the processes of electrodeposition of Ni, Co and Ni-Co alloy powders for all investigated solutions (all Ni^{2+}/Co^{2+} ratios), while corresponding current efficiency versus potential curves for alloy electrodeposition are presented in Fig. 1b, respectively. Current efficiency was obtained from the ratio between the current of alloy electrodeposition and total current [corrected for IR drop—as explained in our next paper (V.D. Jović, B.M. Jović, M.G. Pavlović, in preparation) too]. As can be seen significantly, different polarization curves are obtained. Polarization curves for Ni–Co alloy powder electrodeposition at the ions ratios of 4, 1.5 and 0.67 are positioned between those for pure metals, while the one for the ratio 0.25 overlaps with that for Co. It is interesting to note that the polarization curves for the ratios 1.5 and 0.67 are at the same potential, slightly more positive than that for Ni, while the one for the ratio 4 appears at more positive potentials. Such a behavior indicates that the position of polarization curves do not follow either the ratio of metal ions in the electrolyte or the metal content in the powder deposit (see Fig. 2). A special case is the polarization curve for the ratio 4. Instead of being closest to the one for pure Ni, it is placed at more positive potentials, indicating that such behavior could be the consequence of anomalous codeposition (see "Composition of the Ni–Co alloy powders"). The diffusion limiting currents for polarization curves corresponding to the ions ratios 1.5 and 0.67 are lower than that for pure Co and higher than that for pure Ni, while others two (for ions ratios 4 and 0.25) are much higher than those of pure metals. This phenomenon could partially be explained by the fact that in those two cases (ratios 4 and 0.25), total concentration of metal ions in the electrolyte is for 25% higher (see experimental) than that for other two ratios (1.5 and 0.67) and pure metals. Taking into account that the in-

Fig. 1 a Polarization curves for the electrodeposition of Ni, Co and Ni–Co alloy powders from the solution containing different Ni^{2+}/Co^{2+} ions ratios (marked in the figure) obtained after IR drop correction and subtraction of hydrogen evolution current. **b** Corresponding η_j versus E curves
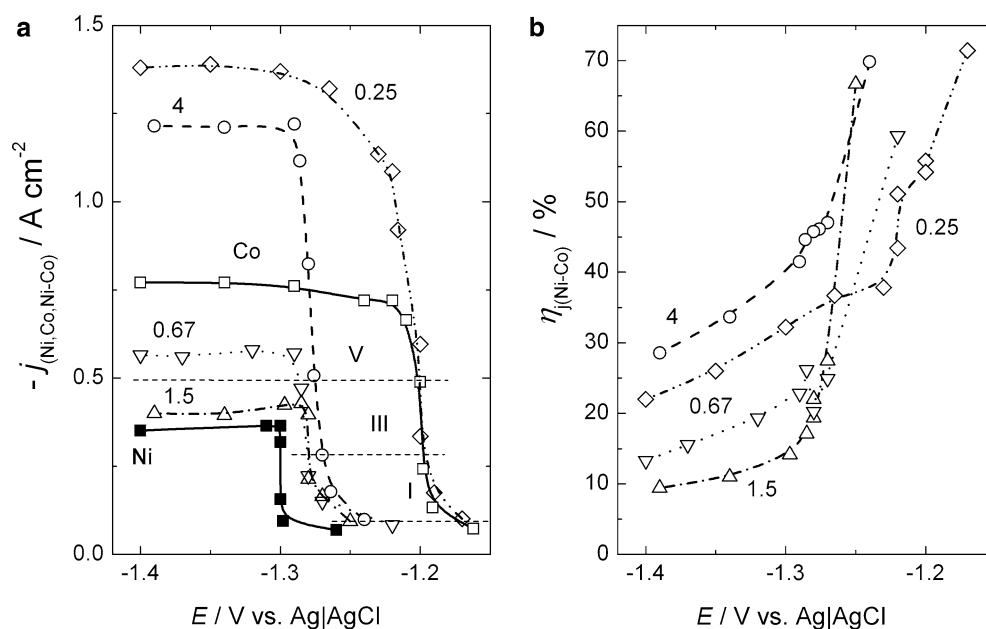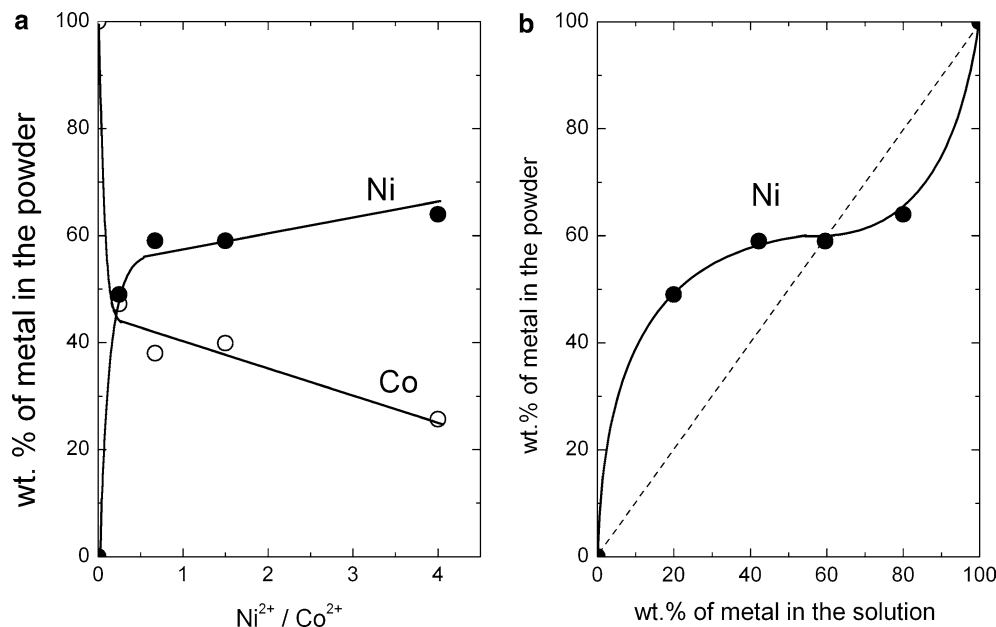
crease of the diffusion limiting current densities is not
proportional to the increase in total ions concentration
for either of those cases (it is much more pronounced for
the ions ratio 4 than 0.25), it is most likely that this
should be explained by the difference in the increase of
the real surface area during the process of electrode-
position. This is in accordance with the fact that about
26 at % of Co codeposited with Ni for the ions ratio 4
(Fig. 2a) follows this ratio and accordingly cannot ac-
count for this effect. At the same time, as can be seen in
Fig. 1b, current efficiency for Ni–Co alloy powder elec-
trodeposition is higher for ratios 4 and 0.25 in com-
parison with those for ratios 1.5 and 0.67, indicating that
the current efficiency increases with the increase of total
metal ions concentration. As can be seen in Fig. 1b al-
ready at the beginning of the deposition process signif-
icant amount of hydrogen is evolving, causing the value
of the current efficiency of about 50–70%. At more
cathodic potentials this value decreases to about 12–
15%, or 20–25% (depending on the metal ions concen-
tration) with the sharp decrease taking place in the re-
gion of the sharp increase in current density.

Finally, it should be noted that dashed lines I, III and
V in Fig. 1a represent values of current density at which
powders were electrodeposited and their morphology
and phase structure investigated.

Composition of the Ni–Co alloy powders

According to the results of the chemical analysis of
electrodeposited powders, the ratio of Ni^{2+}/Co^{2+} ions,
i.e. electrolyte composition, significantly influenced the
composition of electrodeposited powders. It should be
noted here that both elements, Ni and Co were analyzed
independently and that only for the ratio of $Ni^{2+}/Co^{2+}=4$ their sum was not 100%, but about 90%.

The influence of the electrolyte composition on the
alloy powder composition is shown in Fig. 2a and b. As
can be seen in Fig. 2a the content of Ni increases with the
increase in the ratio of Ni^{2+}/Co^{2+} ions, while the con-
tent of Co decreases and both dependences are approx-
imately linear after sharp increase (decrease). According
to Brenner's classification [20], the behavior presented in
Fig. 2b indicates two types of powder co-deposition:
irregular, up to the 60 wt% of Ni (or 40 wt% of Co) in
the solution and anomalous at higher amounts of Ni. The
irregular co-deposition is expected to occur in systems in
which the standard potentials of the parent metals are
close together and with metals that form solid solution.
Both conditions are fulfilled for the system Ni–Co [20,
21]. The characteristic of anomalous co-deposition is that
it occurs only under certain conditions of concentration
and operating variables for a given plating bath [20].
Hence, if the deposition of the more noble metal is so
strongly inhibited that no current can be recorded as the
potential is driven negative, at some potential the more
noble metal would start depositing causing the increase
of deposition current. At some more negative potential,
the breakthrough in deposition of the more noble metal
may happen as a result of reduction or removal of the
additive or by opening some alternative mechanism of
discharge, not operative at less negative potential. Such a
case is found in the deposition of Ni–Zn alloys and is
explained by "the hydroxide suppression mechanism"
[22, 23]. It has already been shown that from simple salt
containing electrolytes co-deposition of Ni and Co pos-
sesses anomalous character [20, 24–26], as well as in the
electrolytes containing metal complexes [27], but in all
cases compact deposits were obtained. As can be seen in
Fig. 2b at the conditions of powder electrodeposition
irregular and anomalous character of Ni and Co co-
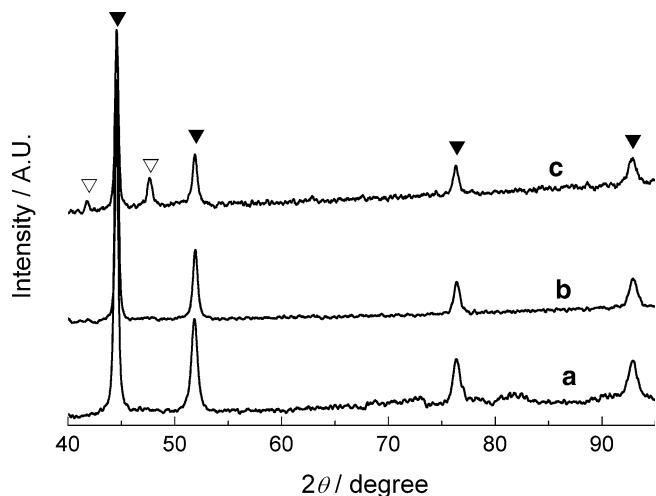deposition are achieved, depending on the solution
composition.

Fig. 3 X-ray diffractograms of Ni–Co powders electrodeposited at a current density of 0.5 A cm^{-2} from the solutions containing different Ni^{2+}/Co^{2+} ions ratio: **a** Ni^{2+}/Co^{2+} = 4.00; **b** Ni^{2+}/Co^{2+} = 1.50; **c** Ni^{2+}/Co^{2+} = 0.67. Peaks for f.c.c. β-Ni phase (▼); peaks for h.c.p. α-Co phase (▽)

Phase structure of the electrodeposited Ni–Co alloy powders

The X-ray diffraction patterns of three samples are shown in Fig. 3. As can be seen XRD patterns contain the characteristic peaks for Ni reach phase, β-Ni phase (▼) with face-centered cubic lattice (f.c.c., space group Fm3m) and h.c.p. α-Co phase (▽). In Table 1 are given details for all phases detected on the Ni–Co alloy powder diffractograms. The full width at half maximum (FWHM) was measured. Crystallite size and lattice distortion were determined on the base of the Cauchy expression: $\beta\cos\theta = K\lambda/D + 4\epsilon\sin\theta$ in which total broadening (β) is the sum of peak broadening due to crystallite size (D) and broadening due to lattice distortion (e) [28, 29]. As can be seen in Fig. 3 and Table 1 with the decrease of Ni^{2+}/Co^{2+} ions ratio, peaks for β-

Ni phase (▼) become smaller and some of them disappear, while the peaks for h.c.p. α-Co phase (▽) become visible (Fig. 3c). For samples electrodeposited from the solutions containing higher concentration of Ni^{2+} than Co^{2+} ions (Ni^{2+}/Co^{2+} = 4.00 and Ni^{2+}/Co^{2+} = 1.50) only the presence of β-Ni phase (▼) was detected, while at concentration ratios Ni^{2+}/Co^{2+} < 1 h.c.p. α-Co phase (▽) together with β-Ni phase was detected in the powder deposit.

It is interesting to note that in comparison with the results of El-Halim et al. [18] phase structure of electrodeposited Ni–Co powders from ammoniacal electrolyte is slightly different. The difference reflects in the finding that only β-Ni phase is detected in Ni–Co alloy powders containing 60–65 wt% Ni, while the mixture of β-Ni and α-Co phases is detected in alloy powders containing 50–60 wt % Ni (Fig. 3). Such a behavior indicates that the formation of β-Ni and α-Co phases is more sensitive to the wt% of metals in the solution, since only β-Ni phase is detected in alloy powders electrodeposited from solutions containing 60–80 wt% Ni, while the mixture of β-Ni and α-Co phases is detected in alloy powders electrodeposited from solutions containing 20–40 wt% Ni. It should also be mentioned here that the composition of the electrolyte in the work of El-Halim et al. [18] was different than that in our work (they used sulfate-boric acid electrolyte) and that this could be the reason for the difference in the X-ray analysis for alloy powders obtained in these two works.

Morphology of the Ni–Co alloy powders

The influence of alloy powder composition

The morphology of Ni–Co alloy powders electrodeposited at the highest current density of j = 0.5 A cm^{-2} from the electrolytes containing different Ni^{2+}/Co^{2+} ions ratio is shown in Figs. 4, 5, 6 and 7. As can be seen the morphology of Ni–Co alloy powder is sensitive to the

Fig. 4 Morphology of Ni–Co powder particles electrodeposited at a current density of 0.5 A cm^{-2} from the solution containing Ni^{2+}/Co^{2+} = 4.00 ions ratio

Fig. 5 Morphology of Ni–Co powder particles electrodeposited at a current density of $0.5 \, A \, cm^{-2}$ from the solution containing $Ni^{2+}/Co^{2+} = 1.50$ ions ratio
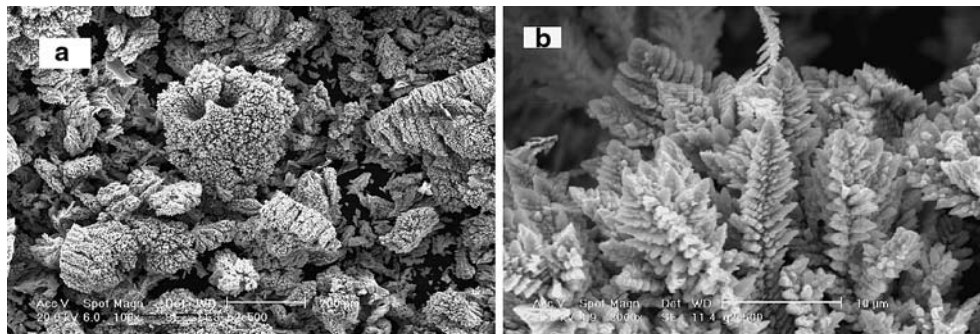
Ni^{2+}/Co^{2+} ions ratio, i.e. to the composition of the alloy powder.

In the powder containing the highest amount of Ni, of about 64 wt% Ni electrodeposited at the $Ni^{2+}/Co^{2+} = 4.00$, more than 90% of particles were typical spongy particles varying in the size from about 50 μm to about 200 μm shown in Fig. 4. Very few cauliflower-like particles of slightly different shape than those typical for pure Ni powder [30] were also detected in the alloy powder. One such particle is marked with the arrow in the upper right corner of Fig. 4. It is important to note that this particle has a flat surface on one side indicating that this type of growth belongs to the beginning of the powder formation, with this particle falling off from the electrode surface before the bigger, typical spongy agglomerate is formed. Spongy particles are more similar to the ones detected in pure Co powder [30], with the presence of large number of cavities, but contrary to the situation in pure Co powder, here practically non of the cavities possess fern-like dendrites on their bottom, indicating that the growth mechanism of alloy powder particles is different than that of pure Co powder [30]. It is interesting that practically no dendrites are found in this powder, although about 26 wt% of Co is present in the powder.

As the Ni^{2+}/Co^{2+} ions ratio in the electrolyte decreases from 4.00 to 1.50 the composition of the Ni–Co alloy powder changes from about 65 wt% Ni–26 wt% Co to about 60 wt% Ni–40 wt% Co (Fig. 2) and this change reflects in the morphology of the powder. All powder agglomerates are covered with the fern-like dendrites (Fig. 5b), few of them are bigger (about 200 μm) and characterized by the presence of cavities with their number being significantly reduced (Fig. 5a)

in comparison with the previous one. As can be seen in Fig. 5a significant number of dendritic particles is detected in this powder deposit (around the agglomerate), contrary to the previous one. Very few spongy-like particles of the size of about 500 μm are also present in the powder and they are also covered with the fern-like dendrites, indicating that in the presence of higher amount of Co in the powder dendritic growth prevails.

It is interesting to note that with further decrease of the Ni^{2+}/Co^{2+} ions ratio in the electrolyte from 1.50 to 0.67 the composition of the Ni–Co alloy powder practically does not change (Fig. 2), although the morphology of powder particles is slightly different. In this case, the number of agglomerates increases in comparison with the previous one, with the shape of agglomerates being different, as can be seen in Fig. 6a and b. The common characteristic of all agglomerates is that they are covered with the fern-like dendrites. At the same time higher amount of dendritic particles (around the agglomerate shown in Fig. 6b) are formed during Ni–Co powder electrodeposition in this case in comparison with the previous one. The size of dendrite particles varies from about 5 μm to about 50 μm.

In the Ni–Co alloy powder deposit with the highest percentage of Co different types of agglomerates could be detected: (1) spongy-like particles of the size of about 500 μm covered with the fern-like dendrites, also found in the previous deposit (Fig. 6b); (2) compact agglomerates, characteristic for pure Co powder deposit (Fig. 7a); (3) agglomerates composed of closely packed fern-like dendrites about 200 μm long (Fig. 7b). By the EDS analysis of the compact agglomerate shown Fig. 7a, it is found that it does not represent pure Co particle, but the Ni–Co alloy of identical composition as

Fig. 6 Morphology of Ni–Co powder particles electrodeposited at a current density of $0.5 \, A \, cm^{-2}$ from the solution containing $Ni^{2+}/Co^{2+} = 0.67$ ions ratio
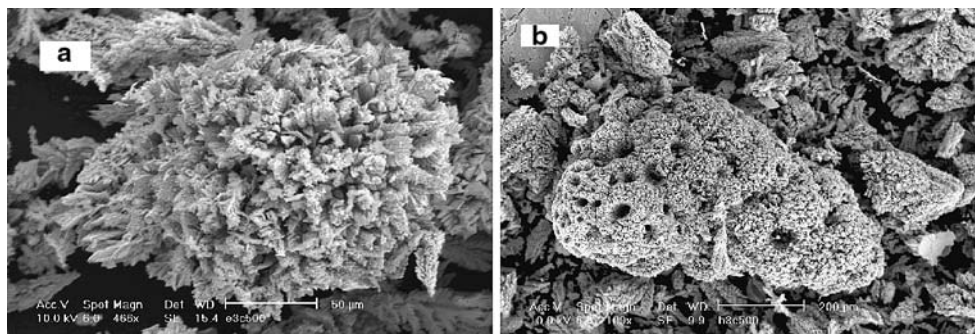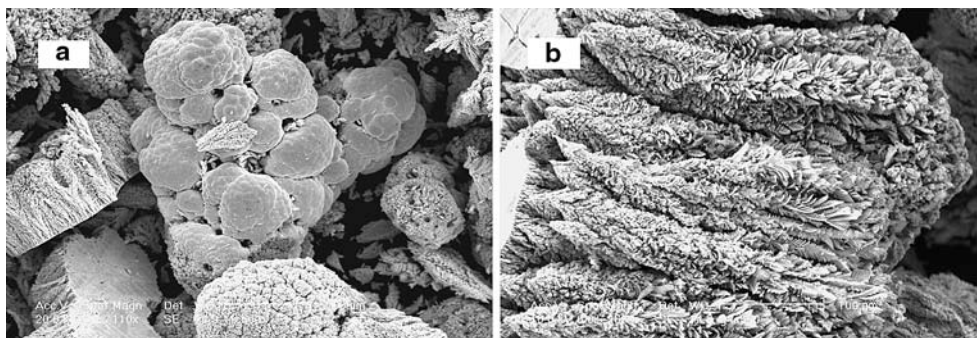
Fig. 7 Morphology of Ni–Co powder particles electrodeposited at a current density of 0.5 A cm^{-2} from the solution containing Ni^{2+}/Co^{2+} = 0.25 ions ratio

the rest of the powder, indicating that the formation of alloy particles follows a growth mechanism for Co powder formation [30].

Considering all detected types of particles in electrodeposited Ni–Co alloy powders of different compositions one can conclude that only one powder (with 65 wt% of Ni) contain very small amount of cauliflower-like particles, typical for pure Ni powder but slightly different, while the rest of them contain some of the particles detected in pure Co powder. The difference between the particles detected in pure Co powder and in Ni–Co alloy powder (except for the particles obtained from the electrolyte with the highest Ni^{2+}/Co^{2+} ions ratio, Fig. 4) is the presence of fern-like dendrites on the surface of these particles. Such a behavior indicates that for these three alloy compositions the presence of Ni^{2+} and Co^{2+} ions promotes dendrite formation on the surface of all particles detected in Ni–Co alloy powders. Hence, it appears that although some similarities between the type of particles (agglomerates) detected in pure Co and Ni–Co alloy powders exists, it is practically not possible to correlate composition of alloy powders with their morphology. Such a behavior could also be the consequence of the fact that two different types of co-deposition of Ni and Co (irregular and anomalous) take place during the Ni–Co alloy powder electrodeposition, as well as that massive hydrogen evolution occurs during the process of alloy electrodeposition.

In order to explain the difference in the morphology as a function of alloy composition (Ni^{2+}/Co^{2+} ions ratio) one should refer to the polarization curves presented in Fig. 1a. As can be seen in this figure at the applied current density of 0.5 A cm^{-2} (dashed line V) only one alloy, electrodeposited at the Ni^{2+}/Co^{2+} = 1.50, deposits at its diffusion limiting current density, the one electrodeposited at the Ni^{2+}/Co^{2+} = 0.67 deposits at a slightly lower current density than its diffusion limiting current density, while for the alloys electrodeposited at Ni^{2+}/Co^{2+} = 4.00 and 0.25 applied current density lies in the region of mixed control of deposition, being much less than the diffusion limiting current density for those electrolyte compositions. Bearing in mind that the currents presented in this figure represent only 20% of the total current (see V.D. Jović, B.M. Jović, M.G. Pavlović, in preparation) and that massive hydrogen evolution takes place together

with the process of alloy electrodeposition, it is quite difficult to find good explanation for the phenomena observed. Different theories concerning powder formation during metal electrodeposition exist in the literature [31] with one of them claiming that powder formation takes place at the diffusion limiting current at potentials of hydrogen evolution, while in this case hydrogen evolution commences already at the beginning of the deposition process being catalyzed by the deposition. Hence, any comparison between these two processes is not realistic, but it is obvious that hydrogen evolution plays an important role in the process of powder electrodeposition.

It should be noted here that there is no agreement between the powder morphology registered in the paper of El-Halim et al. [18] and in this work. The difference could be either due to the different electrolyte composition (sulfate-boric acid, or ammoniacal electrolyte), or the fact that in our work pure powder particles (fallen off from the electrode surface) were analyzed by the SEM, while in the paper of El-Halim et al. [18] deposit that was still on the electrode was investigated.

The influence of the current density on the morphology of Ni–Co powder

After careful investigation of the morphology of Ni–Co alloy deposits obtained at different current densities it seems that the value of current density practically does not influence the morphology, except that the highest amount of about 85% of compact deposit was obtained at the lowest current density of 0.1 A cm^{-2}. Taking into account polarization curves shown in Fig. 1a it is obvious that at this current density, although simultaneous hydrogen evolution occurs, the process of alloy deposition is under "activation" control and that compact deposit should be expected.

Conclusions

From the results presented in this paper it could be concluded that the composition of the electrolyte, i.e. Ni^{2+}/Co^{2+} ions ratio, influences both, phase structure of the alloy powder and its morphology. At the Ni^{2+}/

Co^{2+} ions ratio higher than 1 only β-Ni phase was detected, while at concentration ratios $Ni^{2+}/Co^{2+} < 1$ h.c.p. α-Co phase together with β-Ni phase was detected in the powder deposit. At the highest ratio of Ni^{2+}/Co^{2+} concentration typical spongy particles were obtained. With the decrease of Ni^{2+}/Co^{2+} ions ratio agglomerates of the size of about 100 μm, composed of a large number of fern-like dendrites were obtained. At the lowest Ni^{2+}/Co^{2+} concentration ratio, among more fern-like dendrites, agglomerates typical for pure Co powder deposition were also detected, but they are also Ni–Co alloys. The current density of electrodeposition practically does not influence either the morphology of alloy powder composition. It is also shown that two types of co-deposition of Ni and Co, irregular and anomalous, are detected.

References

1. German RM (1994) Powder metallurgy science, metal powder industries federation, 2nd edn. Princeton, New Jersey
2. Popov KI, Pavlović MG (1993) Electrodeposition of metal powders with controlled particle grain size and morphology. In: White RE et al (eds) Modern aspects of electrochemistry, vol 24, Chap 6. Plenum, New York
3. Elmen GW (1928) J Franklin Inst 206:317
4. Elmen GW (1929) J Franklin Inst 207:583
5. Elmen GW (1935) Elect Eng 54:1292
6. Nicolov I, Darkaoui R, Zhecheva E, Stoyanova R, Dimitrov N, Vitanov T (1997) J Electroanal Chem 429:157
7. Haenen J, Vischer W, Barendrecht E (1986) J Electroanal Chem 208:273
8. Singh RN, Koening JF, Poillerat G, Chartier P (1991) J Electroanal Chem 314:241
9. Heller-Ling N, Prestat M, Gautier JL, Koening JF, Poillerat G, Chartier P (1997) Electrochim Acta 42:197
10. Marco J, Gancedo J, Gracia M, Gautier J, Rios E, Berry F (2000) J Solid State Chem 153:74
11. Carapuca H, Pereira M, Costa F (1990) Mat Res Bull 25:1183
12. King W, Tseung A (1974) Electrochim Acta 19:485
13. Svegl F, Orel B, Hutchins MG, Kalcher K (1996) J Electrochem Soc 143:1532
14. Baydi ML, Poillerat MG, Gautier JL, Rehspringer JL, Koening JF, Chartier P (1994) J Solid State Chem 109:278
15. Baydi ML, Tiwari SK, Sing RN, Rehspringer JL, Chartier P, Koening JF, Poillerat MG (1995) J Solid State Chem 116:157
16. Rasiyah P, Tseung A (1995) J Electrochem Soc 130:2384
17. Rashkova V, Kitova S, Konstantinov I, Vitanov T (2002) Electrochim Acta 47:1555
18. Abd El-Halim, Khalil RM (1986) Surf Coat Technol 27:103
19. Yur'ev BP, Golubkov LA (1969) Trudy – Leningradskii Politekhnicheskii Institut imeni Kalinina MI (published in Russian) 269:14
20. Brenner A (1963) Electrodeposition of alloys; principles and practice. Academic, New York
21. Hansen M, Andrenko K (1958) Constitution of binary alloys. Mc-Graw Hill, New York
22. Despić AR, Jović VD (1995) In: White RE et al (eds) Modern aspects of electrochemistry, vol 27, Chap 2. Plenum, New York
23. Horkans T (1981) J Electrochem Soc 128:45
24. Jepson F, Meecham S, Salt FW (1955) Trans Inst Metal Finish 32:160
25. Young CBF, Struyk C (1946) Trans Electrochem Soc 89:383
26. Schoch EP, Hirsch A (1907) Trans Am Electrochem Soc 11:135
27. Jović VD, Tošić N, Stojanović M (1997) J Electroanal Chem 420:43
28. Lönnberg B (1994) J Mat Sci 29:3224
29. Ziegler G (1978) Powder Met Int 10:70
30. Jović VD, Maksimović V, Pavlović MG, Popov KI (2005) J Solid State Electrochem (in press)
31. Calusaru A (1979) Electrodeposition of powders from solutions. Elsevier, New York